Investigating The Effectiveness of Piezo Stripe Actuators on Flexible Cylinder's Dynamic Response under Vortex-induced Vibrations

Ersegun D. Gedikli
Department of Ocean and Resources Engineering
University of Hawaii at Manoa
Honolulu, United States
egedikli@hawaii.edu

Jason M. Dahl
Department of Ocean Engineering
University of Rhode Island
Narragansett, United States
jmdahl@uri.edu

***Abstract*—In this paper, we investigate the effectiveness of piezo stripe actuators in manipulating the flexible cylinder's dynamic response under vortex-induced vibrations. To do this, we test several low aspect ratio flexible cylinders in a recirculating flow channel where we apply a disruption to the cylinder's response using piezoelectric actuators. In the experiments, we test two cylinders where cylinder 1 is comprised of two piezo stripe actuators bonded at the structural second mode anti-node of a rectangular beam, whereas cylinder 2 is comprised of 3 piezo stripe actuators bonded at the structural third mode anti-node of a rectangular beam. The beam characteristics were identified such that the cylinder would oscillate up to fourth mode in the in-line direction while keeping the cross-flow mode shape constant with first mode. As a result of this study, it is observed that piezo stripes are capable of altering the flow-induced vibration response of the cylinders at different reduced velocities. For example, at low reduced velocities where in-line motions dominate, activation of the second mode in in-line results in a decrease in the total in-line and cross-flow response. In addition, the disruption from the piezo actuators could result in a reduction in the system's higher harmonic frequencies. The fact that a small excitation in one direction can induce significantly different dynamic behaviors in the other direction in the form of vibration reduction or amplification is of special relevance to deep-water offshore marine structures since the flow conditions are generally multi-directional. Another interesting observation is that, a flexible cylinder under uniform flow conditions can excite with even modes in the in-line direction. It is hypothesized that this is because of the asymmetric mass distribution provided by the piezo attachment and cable connections within the cylinder which breaks the total symmetric fluid loading on the cylinder.**

***Index Terms*—vortex-induced vibrations, piezoelectric, dynamic response**

I. Introduction

Vortex-induced vibration (VIV) is an inherent problem seen in many engineering structures such as bridges, transmission lines, offshore wind turbines, marine cables, and risers. These vibrations have a significant potential for damage in the short term, and also affect the fatigue characteristics of the offshore structures, hence, the conditions under which they emerge are of major relevance to the designers and operators of the systems involved [1]–[3]. While much research has been devoted to active and passive systems to control VIV, such as passive geometry changes to the cylinder [4]–[6], active structural control [7]–[9], or active wake control [10], these studies are often aimed only at cancelling vibrations or reducing the vibrations due to fluid-structure interaction (FSI), rather than manipulating the dynamic system to achieve a desired behavior. With particular emphasis on cancelling cross-flow (CF) motions, many of these previous studies have looked at applying control mechanisms that will directly cancel the offending motions. For example, [8] applied piezoelectric actuators to control base excitation of a flexible cylinder only in the CF direction since the predominant motions of the cylinder were in the CF direction.

Recent work showed that spanwise in-line (IL) response of a flexible cylinder is closely tied to the spanwise CF response [11], [12]. In particular, the shape of the IL response of a low-mode number flexible cylinder will pass through several of the IL natural frequencies of the system without changing the in-line shape of the response over a range of reduced velocities, however when the cross-flow response shape changes, the IL response will switch to a shape consistent with the nearest structural mode [12]. This implies a strong coupling between the IL and CF response in a flexible cylinder. Due to the strong coupling, it is hypothesized that any change in one direction should result in a change in the other. In this work, we show the preliminary results of our new experiments in which we test four distinct configurations to gain a better understanding of piezo stripe actuators' efficiency at influencing the dynamic response of cylinders. In particular, we investigate whether a modest perturbation from piezoelectric actuators may be utilized to disrupt the response in both the IL and CF directions individually. This is different than the earlier experiments of [13], where only IL response was tested.

II. Methods

A. Description of The Experimental Setup

Experiments were carried out in a recirculating flow channel to observe the coupled FSI response with and without piezo actuation. The test section of the flow channel has the dimensions of 38 cm wide by 51 cm high by 152 cm length with a

38 cm by 38 cm viewing window located at the downstream of the tank. Top image in Figure 1 illustrates the top view and bottom images illustrate the front view of the flow channel with the experimental set-ups.

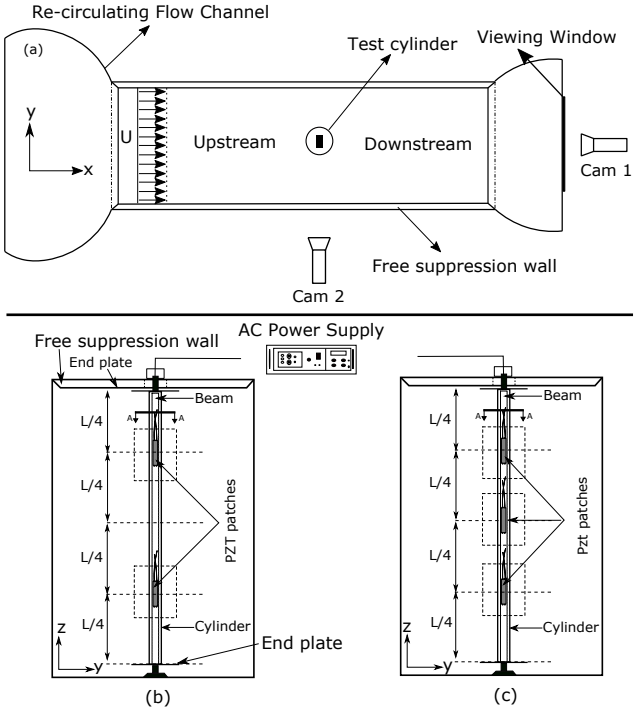

Fig. 1. Sketch of the experimental set-up in recirculating water flow channel. (a) Top view of the experimental set-up with cylinder placed at the center of the test section. (b) Front view of the experimental set-up with piezos bonded at the second mode anti-nodes of the test cylinder. (c) Front view of the experimental set-up with piezos bonded at the third mode anti-nodes of the test cylinder. Water flows in $x-$direction.

Flow channel has the capacity of running experiments up to 1 m/s, but tests were conducted at a lower flow speed range of 0.1-0.6 m/s to minimize the wave formation at the top and also to ensure the current profiles to be uniform over depth. A free suppression wall across the open portion of the flow channel was also constructed at the top of the tank to minimize the wave formation and to ensure the symmetry at the top and the bottom of the cylinder.

In the tests, two cylinders were used to characterize the IL and CF coupled FSI for four different piezo configurations. In the first configuration, two piezos were bonded at the second mode anti-nodes of the cylinder (see Fig. 1b) where fluid flows in the x- direction. In the second configuration, same test cylinder was rotated 90 degrees allowing larger CF oscillations than the first configuration since smaller cross-section of the beam was facing in the CF direction. In the third configuration, a second test cylinder was used. In this configuration, three piezos were bonded at the third mode anti-nodes of the second cylinder (see Fig. 1c). Finally, similar to the second configuration, test cylinder was rotated 90 degrees allowing larger cross-flow oscillations than the third configuration.

In the experiments, test cylinders were attached vertically from the center of the bottom of the tank to the free suppression wall (see Fig. 1). Cylinders were marked with 21 equally spaced white dots in both IL and CF. The distance between each dot was 1.6 cm and two high-speed cameras were used to track the motion of the dots in the flow channel with the sampling frequency of 150 Hz. Camera 1 was placed in front of the the flow channel to capture the motion in the CF and Camera 2 was placed at the side of the viewing tank to capture the motion in the IL. The piezo actuators were excited with a predetermined frequency (determined in in-air experiments) to disrupt the spanwise mode shape of the flexible cylinder where piezo excitation was performed as open loop with no feedback from the motion of the cylinder. In-air experiments were carried for two reasons: 1) to test the hypothesis that piezo actuators are capable of changing the mode shape of the cylinder, and 2) to determine the highest piezo frequencies that provide the most energy to the system. The results of in-air experiments are omitted in this paper for simplicity.

B. System Properties

TABLE I
CYLINDER CHARACTERISTICS AND DIMENSIONLESS PARAMETERS

Variable	Equation	Cylinder 1 (2 Piezo)	Cylinder 2 (3 Piezo)	Units
h	–	0.635	0.635	mm
b	–	3	3	mm
D	–	9.525	9.525	mm
L	–	381	381	mm
f_w	–	4.2	7	Hz
m^*	$4m/(\rho\pi LD^2)$	1.15	1.2	–
AR	L/D	40	40	–
ξ_a	$\delta_a/\sqrt{(\delta_a^2+4\pi^2)}$	0.015	0.022	–
ξ_w	$\delta_w/\sqrt{(\delta_w^2+4\pi^2)}$	0.06	0.019	–
Re	UD/ν	900-5200		–
Vr_n	$U/(f_wD)$	3-13		–
f_s	–	150	150	Hz
f_{IL}				
	Mode 1	0.93	1.55	Hz
	Mode 2	2.59	4.31	Hz
	Mode 3	5.08	8.47	Hz
	Mode 4	8.40	14	Hz
f_{CF}				
	Mode 1	4.2	7	Hz
	Mode 2	11.67	19.44	Hz
	Mode 3	22.9	38.18	Hz
	Mode 4	37.8	63.09	Hz

The test cylinder consisted of a urethane rubber material molded around a rectangular plastic beam to provide the appropriate system stiffness. The beam was designed such that the vortex shedding frequencies would remain close to the first structural mode (half-sinusoid) frequency in IL and CF directions, similar to the way the cylinder characteristics were tuned in [12].

Cylinder characteristics and some non-dimensional parameters have been tabulated in Table I where h represents the IL beam width, b represents the CF beam height, D represents the cylinder diameter, L represents the cylinder length, f_w represents the natural frequency in water, m^* represents mass ratio, AR represents the aspect ratio, ξ_a represents damping ratio in air, ξ_w represents damping ratio in water, Re represents the Reynolds number, Vr_n represents the nominal

reduced velocity. In addition, m represents the cylinder mass, ρ represents material density, δ_w represents the logarithmic decrement obtained from decay tests in water, δ_a represents the logarithmic decrement obtained from decay tests in air, and ν represents kinematic viscosity of the water. Bottom section in Table I shows the designed frequency characteristics for cylinders 1 and 2 representing the systems in Fig. 1. Both cylinders were designed such that cylinder would oscillate up to fourth mode in IL direction keeping the CF response constant with a first mode shape within the flow speed range. Desired structural frequencies are calculated using the natural frequency equation for a fixed-fixed beam assuming the initial vertical tension to be negligible [11], [14]. When designing the desired cylinder frequencies and corresponding mode shapes, it was assumed that a cylinder oscillates with 2 : 1(IL:CF) frequency ratio under lock-in, which is a resonance response condition where the vortex shedding frequency locks into the natural frequency of the bluff body [15], [16].

TABLE II
PIEZO RESPONSES ARE MEASURED FOR SELECTED Vr_n VALUES

Vr_n	2 Piezo IL	2 Piezo CF	Vr_n	3 Piezo IL	3 Piezo CF
3		X	1.80	X	X
3.34			2.01	X	X
3.75	X	X	2.25	X	X
4.25	X	X	2.55	X	X
4.69		X	3.60	X	X
5.5	X		4.63	X	X
6		X	5.17	X	X
6.84	X				
7.72		X			
8.62		X			

III. RESULTS

Experiments in recirculating flow channel were conducted for increased flow speeds between the Reynolds number values of $900 - 5200$ for 22 different flow speeds. To stay within the page limits, we first introduce the maximum amplitude response map and then focus on one flow speed case in all configurations to show the effect of piezo actuation. It should be noted that piezo actuators were not used for all the flow speeds tested (see Table II).

A. Maximum Amplitude Response Map

Figures 2 and 3 show the non-dimensional RMS amplitude response of the Cylinder 1 (two-piezo cylinder) and Cylinder 2 (three-piezo cylinder), and their piezo activated responses at the tested flow speeds. In the figures, black color represents the beam that is oriented in the CF direction, and red color represents the beam that is oriented in the IL direction (in other words the previous cylinder is rotated 90^0). Plus signs represent the piezo activated response amplitude in both IL and CF orientations.

Similar to [17], RMS of the motion time history is calculated for each tracked point along the span. Maximum RMS response shown in Figures 2 and 3 illustrate the maximum value of the RMS over the span. According to Fig. 2 , the

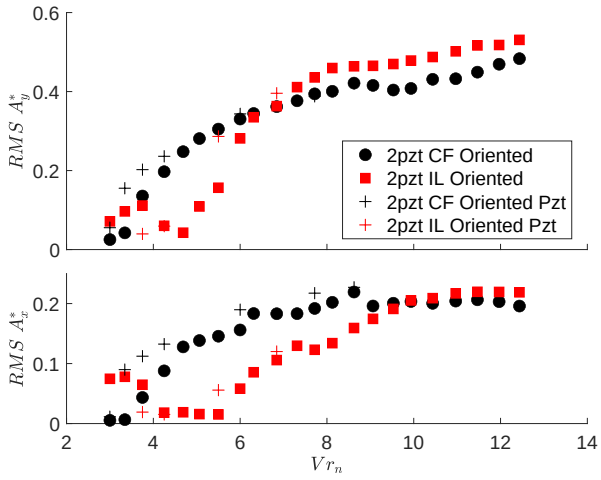

Fig. 2. Non-dimensional RMS CF amplitude (top image) and IL amplitude (bottom image) response of the Cylinder 1 (two-piezo cylinder) where the beams are oriented in CF and IL directions. Black points represent the CF oriented beam, red points represent the IL oriented beam (see Fig. 1). Plus signs represent the piezo activated response of the cylinder.

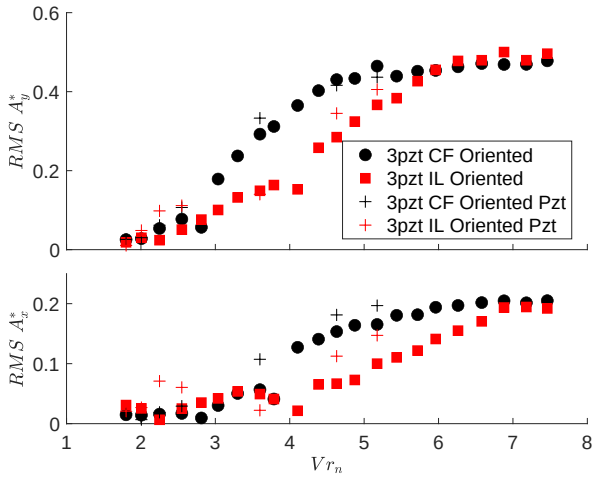

Fig. 3. Non-dimensional RMS CF amplitude (top image) and IL amplitude (bottom image) response of the Cylinder 2 (three-piezo cylinder) where the beams are oriented in CF and IL directions. Black points represent the CF oriented beam, red points represent the IL oriented beam (see Fig. 1). Plus signs represent the piezo activated response of the cylinder.

cylinder oscillates with comparably low amplitudes in IL and CF directions when $4 < Vr_n < 6$ than $Vr_n < 4$ which is an interesting observation where cylinder undergoes resonant state at very low flow speeds. Also, different response regions begin to develop when $4 < Vr_n < 6$ followed by a gradual increase from reduced velocity of 6. Fig. 3 shows that, for the CF oriented three-piezo cylinder, development of response regions occurs for $Vr_n < 3$, with the next region extending until $Vr_n = 4.1$. After that once again we observe a trend of a consistent gradual increase at higher reduced velocities.

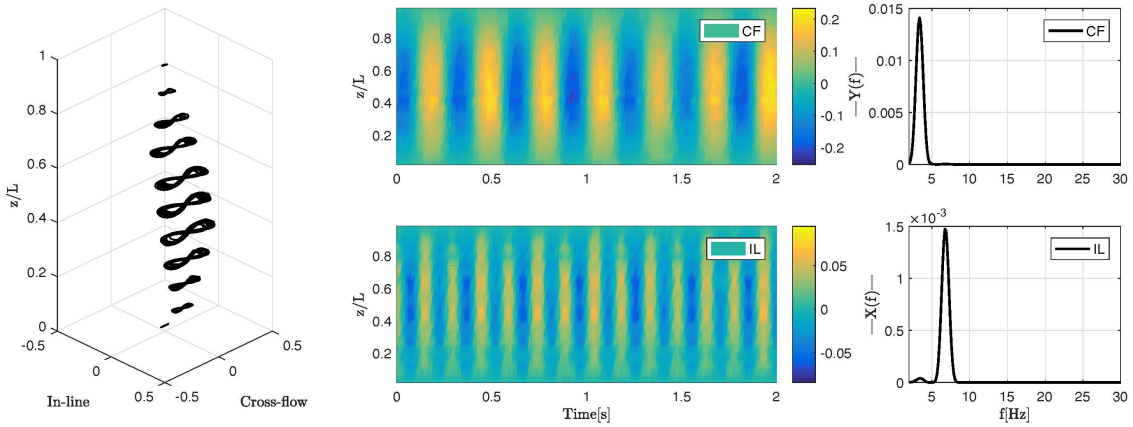

Fig. 4. Two-piezo cylinder oriented in cross-flow before piezo activation. Left: Lissajous shape of the flexible cylinder at $Vr_n = 3.75$ in xy (in-line:cross-flow) plane. Middle Top: Span-wise time history in cross-flow. Right Top: Cross-flow power spectral density. Middle Bottom: Span-wise time history in in-line. Right Bottom: In-line power spectral density.

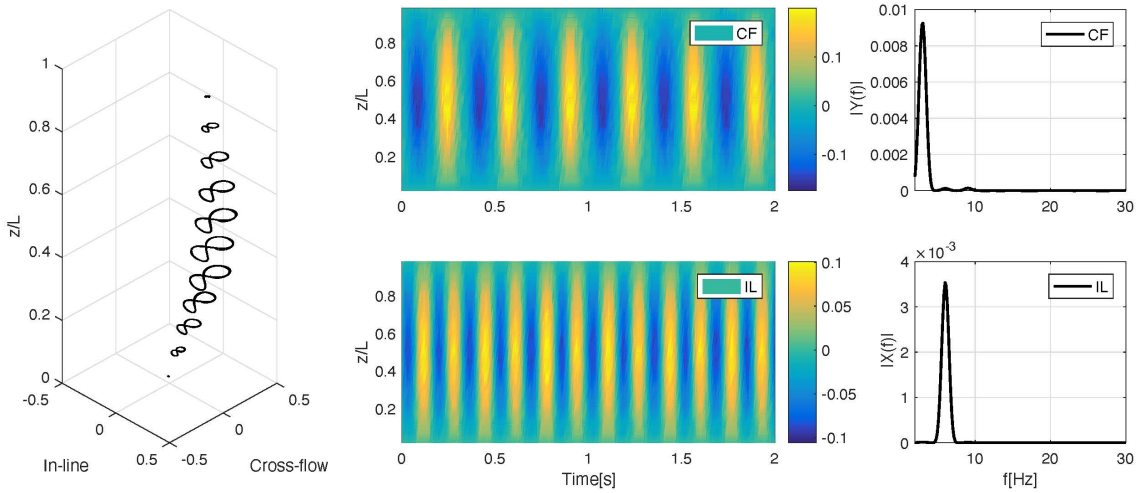

Fig. 5. Two-piezo cylinder oriented in in-line before piezo activation. Left: Lissajous shape of the flexible cylinder at $Vr_n = 3.75$ in xy (in-line:cross-flow) plane. Middle Top: Span-wise time history in cross-flow. Right Top: Cross-flow power spectral density. Middle Bottom: Span-wise time history in in-line. Right Bottom: In-line power spectral density.

B. Dynamic Response at Selected Flow Speeds

For the sake of simplicity and due to page constraints, we will only give the dynamic responses at $Vr_n = 3.75$ where both Cylinders 1 and 2 were tested at this speed.

1) Two-piezo Spanwise Dynamic Response Before Piezo Activation: Figures 4 and 5 illustrate the overall deformation of the two-piezo cylinder with corresponding spanwise time histories and frequency responses at the center of the cylinder: Figure 4 shows the two-piezo cylinder where the beam is oriented in CF and 5 shows the same analysis where the beam is oriented in the IL direction.

Both figures show that the test cylinders are oscillating with a clear figure-eight type of response over the cylinder's span (left image in Figures 4 and 5), and the spanwise time history resembles to a standing wave response (center images in Figures 4 and 5). Center point frequency content confirms that cylinder oscillates with $2:1$ (IL:CF) frequency ratio as illustrated in the right images in Figures 4 and 5. Note that both cylinders oscillate with comparable amplitudes in both in-line and cross-flow directions which are also apparent in Figures 2 and 3.

2) Two-piezo Spanwise Dynamic Response After Piezo Activation: Figures 6 and 7 show the piezo activated response of the same cases at $Vr_n = 3.75$. Figure 6 shows that CF oriented two-piezo cylinder's both cross-flow and in-line responses are enhanced with the piezo activation (also see Fig. 2). There is a small frequency shift in the in-line direction as well as an increase in the total energy of the system. This results in a more pronounced Lissajous shape while maintaining the 2:1 frequency ratio.

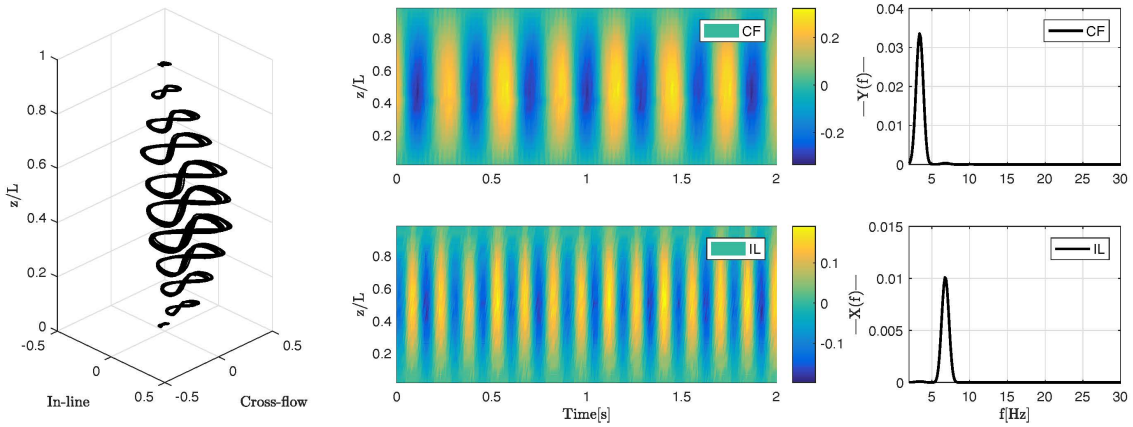

Fig. 6. Two-piezo cylinder where the beam is oriented in cross-flow after piezo activation. Left: Lissajous shape of the flexible cylinder at $Vr_n = 3.75$ in xy (in-line:cross-flow) plane. Middle Top: Spanwise time history in cross-flow. Right Top: Cross-flow power spectral density. Middle Bottom: Spanwise time history in in-line. Right Bottom: In-line power spectral density.

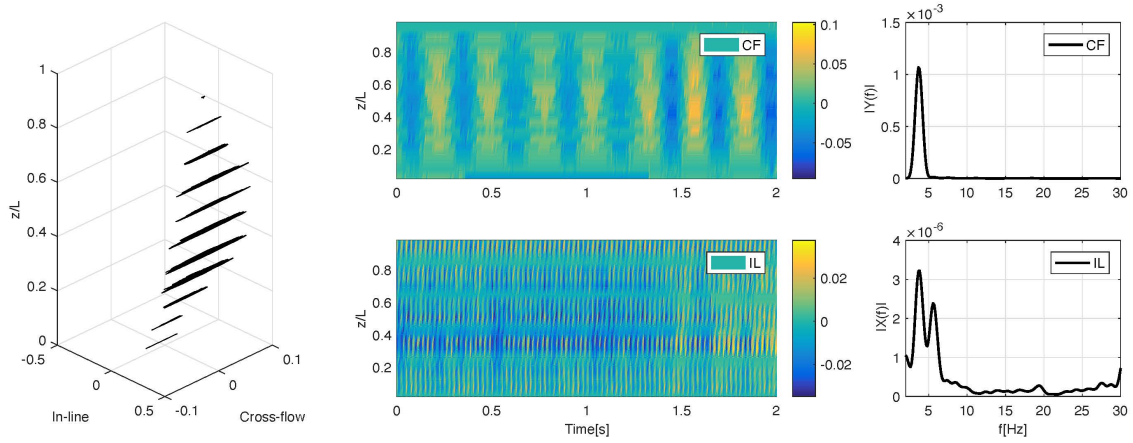

Fig. 7. Two-piezo cylinder where the beam is oriented in in-line after piezo activation. Left: Lissajous shape of the flexible cylinder at $Vr_n = 3.75$ in xy (in-line:cross-flow) plane. Middle Top: Spanwise time history in cross-flow. Right Top: Cross-flow power spectral density. Middle Bottom: Spanwise time history in in-line. Right Bottom: In-line power spectral density.

On the other hand, when the piezos are oriented facing the IL, an almost complete suppression of IL motion occurs which also results a large decrease in non-dimensional amplitude in the CF direction as shown in Fig. 7. In other words, most of the energy was removed from the system by activating the IL piezos which resulted a low-amplitude response as in Fig. 7.

It is also important to note that the mode shapes in the IL orientation varied significantly within the flow speed range tested, whereas no significant mode shape variation was observed in the CF (not shown). This is also an expected response since the cylinder were designed to oscillate with higher order modes in the IL directions (see Table I). For instance, several dominant IL mode responses were found at low reduced-velocity values up to $Vr_n = 6.5$ for cylinder 1, where the cylinder oscillated in a variety of modes up to fourth mode (although the cylinder's overall IL response between the reduced velocities of 4 and 6 was insignificant as shown in Fig. 2), however the modal response settled to a first mode shape at higher flow speeds. Within the same flow speed range, spatial CF response was always identical to dominant first mode.

IV. Discussion

The study can be discussed based on two different aspects: first, the cylinder's dynamic response without piezo activation and second, manipulating the cylinder dynamics with the use of piezo actuators. The dynamic response of the beam-dominated cylinder experiments showed that an asymmetric response (even mode excitations) is possible in IL at low Reynolds number values despite the earlier findings of [18]–[20]. However, it is important to remember that even though cylinder is attached symmetrically at the top and bottom of the cylinder, piezo attachment and cable connections within the cylinder provide an asymmetric mass distribution which in turn breaks the total symmetric fluid loading on the cylinder. Therefore, natural symmetric loading provided by the recircu-

lating uniform flow channel does not exist in this set-up. This must be further investigated.

Another important observation from the present experiments is that in uniform flow conditions, the cylinder could excite with different modes in the IL direction keeping the CF motion constant, and these mode variations in IL may be controlled through the use of piezo stripe actuators.

Previously, [8] used a flexible cylinder with clamped-free boundary condition in air and bonded the piezo actuators at the bottom of the cylinder to control the dominant mode of vibration. Later, [7] used piezo actuators as an external energy source on a rigid square cylinder which was allowed to move only in the CF direction in air. In the current study, the experimental approach to control/ manipulate the VIV response was carried out in two ways: 1) piezo stripe actuators were activated before a spatial mode change thus tripping the frequency and forcing the cylinder to excite with a higher mode hence vibration suppression (see Fig. 8), 2) piezo actuators were activated right before and apparent amplitude increase, thus forcing the cylinder to jump to higher amplitude response regime hence vibration enhancement (see Fig. 2). Figure 8 shows an example vibration reduction that occurred for the the IL facing two-piezo cylinder (cylinder 1). In the figure, the image at the left illustrates the cylinder's IL spatial response, the center image represents the CF response, and three images at the right illustrate the Lissajous shapes at three different locations across the cylinder's span.

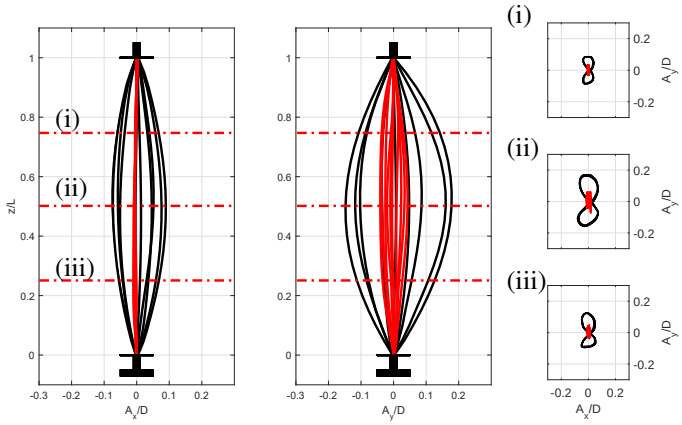

Fig. 8. Piezo activated dynamic response of the test cylinder 1 at $Vr_n = 3.75$ and resulting Lissajous shapes at three different locations across it's span. Black motion response indicates the motion before the piezo actuation, and red motion response indicates the motion after the piezo actuation.

Initial results and analysis show that a flexible cylinder vibration in VIV can be manipulated to change the cylinder's state in two ways: 1) piezo excitation provides additional energy input and forces cylinder to change it's spatial mode shape, 2) the extra energy input either increases (vibration enhancement) or decreases (vibration suppression) the amplitude with no apparent impact on the modal response as shown in Figures 2 and 3 (this is most likely due to the piezo not being able to give enough energy to the cylinder to cause a modal change at higher flow rates).

REFERENCES

[1] T. Sarpkaya, "A critical review of the intrinsic nature of vortex-induced vibrations," *Journal of Fluids and Structures*, vol. 19, no. 4, pp. 389–447, 2004.

[2] P. W. Bearman, "Vortex Shedding from Oscillating Bluff Bodies," *Annual Review of Fluid Mechanics*, vol. 16, no. 1, pp. 195–222, 1984, _eprint: https://doi.org/10.1146/annurev.fl.16.010184.001211. [Online]. Available: https://doi.org/10.1146/annurev.fl.16.010184.001211

[3] C. Williamson and R. Govardhan, "Vortex-Induced Vibrations," *Annual Review of Fluid Mechanics*, vol. 36, no. 1, pp. 413–455, 2004, _eprint: https://doi.org/10.1146/annurev.fluid.36.050802.122128. [Online]. Available: https://doi.org/10.1146/annurev.fluid.36.050802.122128

[4] R. D. Blevins, *Flow Induced Vibrations*, 2nd ed. Van Nostrand Reinhold Company, New York, NY, 1990.

[5] M. Zdravkovich, "Review and classification of various aerodynamic and hydrodynamic means for suppressing vortex shedding," *Journal of Wind Engineering and Industrial Aerodynamics*, vol. 7, no. 2, pp. 145 – 189, 1981.

[6] M. F. Unal and D. Rockwell, "On vortex formation from a cylinder. part 2. control by splitter-plate interference," *Journal of Fluid Mechanics*, vol. 190, p. 513 – 529, 1988.

[7] L. Cheng, Y. Zhou, and M. Zhang, "Perturbed interaction between vortex shedding and induced vibration," *Journal of Fluids and Structures*, vol. 17, no. 7, pp. 887 – 901, 2003.

[8] A. Baz and M. Kim, "Active modal control of vortex-induced vibrations of a flexible cylinder," *Journal of Sound and Vibration*, vol. 165, no. 1, pp. 69 – 84, 1993.

[9] J. F. Williams and B. Zhao, "The active control of vortex shedding," *Journal of Fluids and Structures*, vol. 3, no. 2, pp. 115 – 122, 1989.

[10] S. Rashidi, M. Hayatdavoodi, and J. A. Esfahani, "Vortex shedding suppression and wake control: A review," *Ocean Engineering*, vol. 126, pp. 57 – 80, 2016.

[11] E. D. Gedikli and J. M. Dahl, "Mode shape variation for a low-mode number flexible cylinder subject to vortex-induced vibrations," in *ASME 2014 33rd International Conference on Ocean, Offshore and Arctic Engineering*. American Society of Mechanical Engineers, 2014, pp. V002T08A071–V002T08A071.

[12] E. D. Gedikli, D. Chelidze, and J. M. Dahl, "Observed mode shape effects on the vortex-induced vibration of bending dominated flexible cylinders simply supported at both ends," *Journal of Fluids and Structures*, vol. 81, pp. 399 – 417, 2018. [Online]. Available: http://www.sciencedirect.com/science/article/pii/S088997461730782X

[13] E. D. Gedikli, D. Chelidze, and J. Dahl, "Active control of flexible cylinders undergoing vortex-induced vibrations using piezo stripe actuators," in *Structural Health Monitoring, Photogrammetry & DIC, Volume 6*. Springer, 2019, pp. 63–65.

[14] E. D. Gedikli, D. Chelidz, and J. Dahl, "Empirical mode analysis identifying hysteresis in vortex-induced vibrations of a bending-dominated flexible cylinder," *International Journal of Offshore and Polar Engineering*, vol. 30, no. 02, pp. 186–193, 2020, publisher: International Society of Offshore and Polar Engineers.

[15] J. Dahl, F. Hover, and M. Triantafyllou, "Two-degree-of-freedom vortex-induced vibrations using a force assisted apparatus," *Journal of Fluids and Structures*, vol. 22, no. 6, pp. 807–818, 2006.

[16] J. Dahl, F. Hover, M. Triantafyllou, and O. Oakley, "Dual resonance in vortex-induced vibrations at subcritical and supercritical reynolds numbers," *Journal of Fluid Mechanics*, vol. 643, pp. 395–424, 2010.

[17] E. D. Gedikli, D. Chelidze, and J. M. Dahl, "Bending dominated flexible cylinder experiments reveal insights into modal interactions for flexible body vortex-induced vibrations," in *The 28th International Ocean and Polar Engineering Conference*. International Society of Offshore and Polar Engineers, 2018.

[18] E. D. Gedikli and J. M. Dahl, "Mode excitation hysteresis of a flexible cylinder undergoing vortex-induced vibrations," *Journal of Fluids and Structures*, vol. 69, pp. 308 – 322, 2017. [Online]. Available: http://www.sciencedirect.com/science/article/pii/S0889974616303188

[19] J. Vandiver and J.-Y. Jong, "The relationship between in-line and cross-flow vortex-induced vibration of cylinders," *Journal of Fluids and Structures*, vol. 1, no. 4, pp. 381–399, 1987.

[20] E. D. Gedikli, J. M. Dahl, and D. Chelidze, "Multivariate analysis of vortex-induced vibrations in a tensioned cylinder reveal nonlinear modal interactions," in *10th International Conference on Structural Dynamics*. Eurodyn, 2017.